Astron. Astrophys. 351, 963–972 (1999)

ASTRONOMY AND ASTROPHYSICS

Orbital elements and abundance analyses of the double-lined spectroscopic binary α Andromedae

T.A. Ryabchikova[1], **V.P. Malanushenko**[2,3], **and S.J. Adelman**[4,5]

[1] Institute of Astronomy, Russian Academy of Sciences, Pyatnitskaya str. 48, 109017 Moscow, Russia
[2] Crimean Astrophysical Observatory, 334413 Nauchny, Crimea, Ukraine
[3] Isaac Newton Institute of Chile, Crimean Branch
[4] Department of Physics, The Citadel, 171 Moultrie Street, Charleston, SC 29409, USA
[5] Visiting Observer, Dominion Astrophysical Observatory, National Research Council of Canada

Received 24 November 1998 / Accepted 6 May 1999

Abstract. We performed a spectroscopic study of the SB2 Mercury-Manganese star α And with Reticon and CCD spectra obtained at the Crimean and the Dominion Astrophysical Observatories. Our measurements particularly of the secondary's radial velocities resulted in improved orbital elements with a spectroscopic mass ratio $m_{\rm B}/m_{\rm A}$ = 0.50 $\pm$ 0.03 which is in good agreement with the mass-luminosity solution for this system. Elemental abundance analyses using synthetic spectra show that the primary has elemental abundances somewhat similar to those of other HgMn stars while the cooler secondary probably is a metallic-line star. The possible variability of Hg II λ3984 is discussed.

Key words: stars: abundances – stars: atmospheres – stars: chemically peculiar – stars: binaries: spectroscopic – stars: individual: α And

1. Introduction

α Andromedae (HD 358 = HR 15) is a bright well-known binary with a Mercury-Manganese (HgMn) primary. Compared with the sharp-lined SB2 systems HR 4072 A, B (Adelman 1994), χ Lup A, B (Wahlgren et al. 1994), 112 Her A, B (Ryabchikova et al. 1996), and 46 Dra A, B (Adelman et al. 1998), α And A and B have wide spectral lines. α And has been known to a SB1 system since 1907 (Ludendorf 1907, Baker 1908) with an orbital period P = $96^d.6960$ (Aikman 1976). Pan et al. (1992) obtained its visual orbit from Mark III Stellar Interferometer observations. They found the orbital elements, the light ratios for λ5500 and λ8000, and a mass ratio of 0.48. Their values closely agree with the best spectroscopic orbital elements (Aikman 1976). With a two magnitude difference in brightness between the components, the lines of the secondary were detected only by a careful study of high S/N CCD spectra by Tomkin et al. (1995) who also measured the secondary's radial velocities near the nodes and calculated spectroscopic orbital elements of this SB2 system. Their elements differ slightly from previous results. But their derived mass ratio of 0.42 $\pm$ 0.02 gives too large a mass for the primary.

Khokhlova et al. (1969), Kodaira & Takada (1978), Heacox (1979), Derman (1982), and Ljubimkov & Polosukhina (1988) performed abundance analyses for α And with photographic spectra. α And A, one of the hottest HgMn stars, has great overabundances of Mn, P, Ga, and Hg, which are typical for such peculiar stars. Our abundance analysis based on high resolution high S/N Reticon and CCD spectra continues our systematic abundance studies of SB2 systems with HgMn primaries. We measured the radial velocities for both stars and obtained more accurate orbital parameters including the mass ratio. Then we combined them with the visual orbit and derived the physical characteristics of both stars. Finally we performed abundance analyses for both components by spectral synthesis.

Send offprint requests to: V. Malanushenko

2. Observations and radial velocity measurements

α And was observed in 1990–91 and 1996–97 at the Crimean Astrophysical Observatory (CrAO) and in 1992–94 and 1997–98 at the Dominion Astrophysical Observatory (DAO). CrAO spectra were obtained with the Coudé spectrograph of the 2.6 m telescope and a CCD detector in spectral regions centered at $\lambda\lambda$4960, 6347 and 6678 with a spectral resolution of around 40000. Typically 3–4 spectra were averaged to get a resultant S/N $\geq$ 300.

DAO Reticon spectra with a reciprocal dispersion of 2.4 Å mm^{-1} and a typical S/N of 200 were obtained for a grid of central wavelengths between λ3830 and λ5180 with 55-Å offsets. A DAO 20 Å mm^{-1} CCD spectrum was used to measure the Hγ line profile. Recently we obtained additional CCD spectra centered at 3970 Å. We used a scattered light correction of 3.5% at the continuum level (Gulliver et al. 1996) and flat-fielded spectra with the exposures of an incandescent lamp placed in the Coudé mirror train. As the substantial rotational velocities of both components make it quite difficult to properly place the continuum, we used synthetic spectra of the binary to find line-free spectral windows. Then we made a polynomial fit of typically 3nd order to normalize the spectra.

We measured the radial velocity of the primary by cross-correlating the observations with synthetic spectra, calculated with the model atmosphere and abundances discussed below. Our errors conservatively estimated to be $\pm$ 2 km s^{-1} depend mainly on inaccuracies in the wavelengths of Mn II lines, the severe blending due to rapid rotation of the primary, and to the distortion of some line profiles by the weak wide features of the secondary. For the primary we found $v \cdot \sin i$ = 52 km s^{-1}.

Radial velocity measurements of the secondary star require a very accurate representation of the primary's spectrum and are more complex as it is 2 mag. fainter than the primary (Pan et al. 1992). Our main source for line data was VALD (Piskunov et al. 1995), which includes Kurucz's (1992) extensive line lists GFIRON, BELLLIGHT, BELLHEAVY, and NIST compilations, for example, Martin et al. (1990). Our spectra showed a blend of three strong Fe I lines at λ4957.5 of the secondary which were only marginally blended with very weak lines of the primary. But even this very strong feature in an A3 V star has a residual intensity of 0.99 in the observed spectrum of α And (see Fig. 6 in Sect. 5). Therefore high S/N spectra are needed for the RV measurements. We also used other strong spectral lines found in an A3 V star spectrum Si II λ6347, Ca II λ3933, Fe I λ4045, Sr II λ4215, and the Fe II-Ti II blend at λ4549.

We weighted a rotationally broadened synthetic spectra of the primary by the light ratio, shifted it by the primary's radial velocity, and then subtracted it from the observed spectrum. The residual spectrum which should only be due to the secondary was then normalized. For the secondary we found its rotational velocity $v \cdot \sin i = 110 \pm 5$ km s^{-1}. The accuracy of RV values for the secondary, which were found by cross-correlation, depends on the quality of our synthetic spectrum. A careful investigation of $\lambda\lambda$4930-60 shows that the formal error for the unblended primary's line λ4953 is 0.6 km s^{-1} . When we used the whole spectral region, the cross-correlation function is asymmetric and the error lies between 1 and 2 km s^{-1} for the primary. A change in the $v \cdot \sin i$ value within our error limits introduces a negligible error of less than 0.2 km s^{-1}. Temperature and abundance variations are correlated. For any temperature within the error limits we get a corresponding abundance, but the form of the synthetic spectrum does not change. A typical error of our cross-correlation procedure for the secondary is 2.2 km s^{-1}. For other spectral regions the typical error is two times larger. Hence we used 5 km s^{-1} as the error estimate for all RV measurements of the secondary.

Table 1 lists the heliocentric Julian dates of the mid-points, the central wavelengths, and the measured radial velocities of each observations. Fig. 1 shows the observed and computed binary spectra in the λ4960 spectral region for a few orbital phases in the rest frame of the primary. The secondary's contribution is shown by dashed lines.

3. Orbital elements

We calculated the orbital elements for α And with a code by Tokovinin (1992) by combining our measurements with those from Abt & Snowden (1973), Aikman (1976), and Tomkin et al.

Table 1. α And observational data

Midpoint (HJD)		Radial Velocity (km s^{-1})	
2400000+	Central λ (Å)	Primary	Secondary
48116.454	6347	1.5	-38.2
48136.368	6347	24.2	
48252.318	6347	-34.6	56.3
48547.335	6347	-38.2	49.8
48548.505	6347	-36.7	42.7
48549.458	6347	-38.7	34.8
48846.016	4685	-33.3	
48847.842	3860	-30.3	
48849.942	4080	-30.9	
48850.982	4630	-30.4	
48851.979	4795	-30.0	
48852.982	4850	-28.4	
48853.983	5180	-24.9	
48856.012	4960	-26.4	10.1
48940.660	4740	-36.1	
49200.964	4190	22.9	-83.4
49202.914	3915	22.1	-84.1
49275.782	4300	0.1	
49276.772	4135	1.6	
49277.679	4410	0.4	
49278.706	4025	1.1	-41.7
49279.693	3970	3.2	
49531.946	4520	-27.7	
49535.960	4740	-24.0	
49538.977	4575	-25.5	3.3
49539.948	4465	-21.5	
49618.812	4245	-31.8	
49621.774	4355	-31.7	
50056.420	6347	6.7	-52.4
50364.415	4960	26.3	-70.6
50364.425	6347	26.4	-62.3
50365.433	6347	25.8	-63.2
50376.274	4960	-27.7	4.8
50381.445	4960	-39.6	36.3
50386.372	6347	-39.9	42.7
50386.378	6678	-41.3	
50386.435	4960	-40.7	35.9
50388.149	6678	-41.3	
50388.353	6347	-37.9	36.1
50388.386	4960	-38.2	40.5
50393.395	4960	-33.9	31.6
50393.400	6347	-34.2	43.8
50401.418	4960	-28.3	19.5
50462.167	4960	24.6	-97.9
50462.177	6347	25.0	-86.6
50473.155	6347	-29.6	1.3
50473.176	4960	-30.8	15.2
50501.194	4960	-27.5	11.5
50501.210	6347	-26.4	5.5
50649.967	5015	21.4	-75.0
50676.910	Hγ	-33.8	
50985.854	3970	-24.8	
51000.913	3970	-12.0	

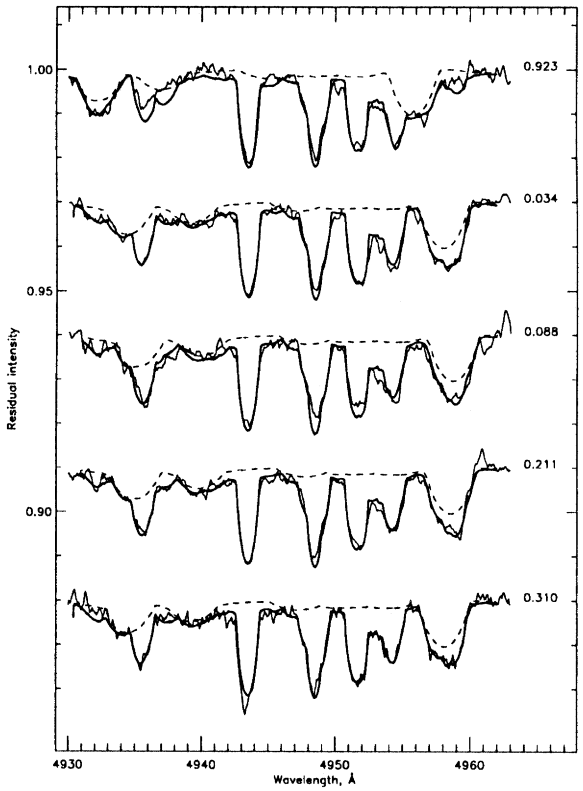

Fig. 1. Comparison of the observed (thin line) and the synthesized (thick line) spectra of α And in the λ4960 spectral region for different orbital phases. The secondary's contributions are shown by dashed lines. The intensity scale is given for the upper spectrum with 0.03 offsets between pairs of spectra.

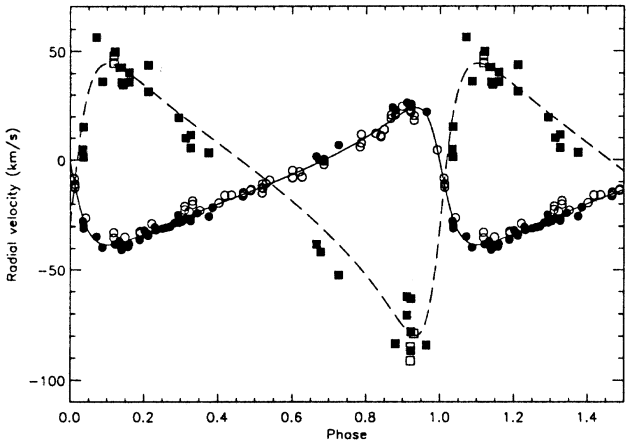

Fig. 2. Radial-velocity curves for the primary (circles) and the secondary (squares). Our measurements are represented by filled symbols, those from other papers by open symbols. Our orbital solution is shown by the solid (primary) and dashed (secondary) lines.

(1995). We weighted values according to our estimated uncertaintes for the primary (2 km s^{-1}) and the secondary (5 km s^{-1}). These 113 values include our 53 measurements from Table 1. Table 2 compares the derived orbital elements of Aikman (1976), Pan et al. (1992) from the visual orbit, Tomkin et al. (1995), and the present study.

The standard deviations of the fit for the primary and the secondary are 2.4 and 9.1 km s^{-1}, respectively, which agree with the adopted accuracies of the radial velocity measurements. Within 2σ our orbital parameters values agree with all previous results. Our orbit-based masses, which were derived using the inclination angle from the visual orbit solution, yield a mass ratio 0.50 $\pm$ 0.03. Tomkin et al. (1995) showed that consistancy between the orbit-based masses and masses from the mass-luminosity solution for α And may be obtained for a mass ratio 0.48 which is close to our value. Their masses are for α And A 3.9–4.0$M_\odot$ and for α And B 1.9–2.0$M_\odot$, but they noted that their spectroscopically obtained mass ratio of 0.42 is not reliable. Combining the last values with our results and with the masses from Pan et al. (1992) we finally adopted $m_A = 3.8 \pm 0.2 M_\odot$ and $m_B = 1.85 \pm 0.13 M_\odot$.

Our γ-velocity is consistent with all previous values except for Abt & Snowden's (1973) γ = -9.6 km s^{-1}. However they measured radial velocities using hydrogen lines which may be somewhat influenced by the contribution of the secondary. Fig. 2 shows the radial-velocity curves for both components of α And. Please note a systematic deviation of the observed secondary's RV from the orbital solution for a few phases. The orbital solutions made separately for both components agree within 2 σ. To check the reality of the systematic deviation of the secondary's radial velocities we repeated the orbit calculations with the radial velocities weighted according to their uncertainties, e.g. 2.4 km s^{-1} for the primary and 9.1 km s^{-1} for the secondary. The derived orbital elements agree with those from Table 2 within less than 1 σ.

Combining our values of $a_1 \sin i$ and $a_2 \sin i$ with the inclination from the visual orbit we obtain a = 0.72 $\pm$ 0.01 au. Using the Hipparcos parallax, 33.6 mas (ESA 1997), we find an orbital angular diameter of $a'' = 0''.0242 \pm 0''.0003$ which is in an excellent agreement with the angular size $a'' = 0''.02415 \pm 0''.00013$ obtained from the visual orbit (Pan et al. 1992).

4. Parameters of the stellar components

Published effective temperatures and surface gravities of α And include 13800 K, 4.00 (Heacox 1979), 13850 K, 3.85 (Derman 1982), and 13700 K, 3.75 (Ljubimkov & Polosukhina 1988). Spectrophotometry (Adelman & Pyper 1983) gives $T_{\rm eff}$ = 13700 K for Balmer jump region and $T_{\rm eff}$ = 10200 K for the Paschen continuum. The infrared flux method gives too small a temperature for α And $T_{\rm eff}$ = 11300 K (Shallis & Blackwell 1979), $T_{\rm eff}$ = 12200 (Glushneva 1987) as the cooler secondary's contribution was not considered. Thus the stellar radius R = 3.98 $R_\odot$ of Shallis et al. (1985) is certainly overestimated. Babu & Shylaja (1981) used a more realistic effective temperature in the infrared flux method for their angular diameter and radius determinations. Their radius value, corrected for the improved parallax (Shallis et al. 1985), is R = 2.7 $R_\odot$.

Effective temperatures and surface gravities of the components of α And were obtained by fitting the observed spec-

Table 2. Orbital elements of α And

	Aikman(1976) Spectroscopy	Pan et al.(1992) Mark III + Spectr.	Tomkin et al.(1995) Spectroscopy	Present Spectroscopy
P(days)	96.6960 $\pm$ 0.0013	96.6960	96.6963 (fixed)	96.7041 $\pm$ 0.0031
T(JD2400000+)	42056.32 $\pm$ 0.20	47374.77 $\pm$ 0.15	49212.17 $\pm$ 0.20	48245.40 $\pm$ 0.24
e	0.521 $\pm$ 0.008	0.527 $\pm$ 0.004	0.60 $\pm$ 0.02	0.555 $\pm$ 0.013
$\omega(^\circ)$	$77^\circ.1 \pm 1^\circ.3$	$77^\circ.31 \pm 1^\circ.32$	$74^\circ.9 \pm 1^\circ.3$	$78^\circ.2 \pm 1^\circ.5$
K_1(km s^{-1})	30.8 $\pm$ 0.3	...	27.8 $\pm$ 0.6	31.2 $\pm$ 0.5
K_2(km s^{-1})	...	...	66.2 $\pm$ 3.6	62.8 $\pm$ 1.5
γ(km s^{-1})	-11.6 $\pm$ 0.2	...	-10.1 $\pm$ 0.2	-10.6 $\pm$ 0.3
$i(^\circ)$	...	$105^\circ.66 \pm 0^\circ.22$	...	...
$a_1 \sin i$ (au)	0.234 $\pm$ 0.002	...	(0.198 $\pm$ 0.004)	0.239 $\pm$ 0.003
$a_2 \sin i$ (au)	...	...	0.558 $\pm$ 0.031	0.482 $\pm$ 0.010
m_A	...	3.8	5.5 $\pm$ 0.5	3.60 $\pm$ 0.20
m_B	...	1.8	2.3 $\pm$ 0.2	1.78 $\pm$ 0.08

trophotometry (Adelman & Pyper 1983) and our Hγ profile. Pan et al. (1992) derived the flux ratio for two wavelengths: 0.160 $\pm$ 0.005 at λ5000 and 0.188 $\pm$ 0.006 at λ8000. Our initial atmospheric parameters for the primary were from Ljubimkov & Polosukhina (1988). Small changes in the secondary's gravity do not greatly influence the fitting of both spectrophotometry and hydrogen line profiles. The best compromise between the spectrophotometry, the observed flux ratio, and the Hγ line profile is achieved with the following parameters:

Primary: $T_{\rm eff}$ = 13800 K, $\log\ g$ = 3.75, [M/H] = +0.2

Secondary: $T_{\rm eff}$ = 8500 K, $\log\ g$ = 4.0, [M/H] = +0.2

The radii ratio from the flux ratio and model fluxes is 1.53. For single bright stars with temperatures close to that of α And, fitting spectrophotometry and the Hγ profile yields errors of $\pm$125 K in $T_{\rm eff}$ and $\pm$0.15 dex in $\log\ g$. As the primary is much brighter than the secondary, these values are appropriate for the primary. From the process of deriving the parameters of the secondary we found that its errors are about twice as great.

Fig. 3 shows the observed and calculated Hγ line profiles for α And while Fig. 4 the observed and the calculated flux distributions. The predictions well fit the spectrophotometry, whose effective bandwidth is 17 Å , except near Balmer line cores where the emergent flux is strongly wavelength dependent. The difficulties in getting a good fit for the Hα region with the rest of the spectrophotometry has also been seen in single stars and may be due to systematic errors. The agreement for the Hγ profile is quite good. The secondary's contribution is relatively small.

Evolutionary tracks by Schaller et al. (1992) provide the luminosities and ages for both components of α And given the adopted masses and effective temperatures:

Primary: $\log(L/L_\odot)$ = 2.38 $\pm$ 0.14, t = $6{\cdot}10^7$ yr

Secondary: $\log(L/L_\odot)$ = 1.10 $\pm$ 0.2, t = $7{\cdot}10^7$ yr

Both stars are near the Zero Age Main Sequence. Applying Bolometric corrections (Flower 1996) we get absolute magnitudes -0.19 $\pm$ 0.30 mag and +2.00 $\pm$ 0.30 mag for the primary and the secondary, respectively, which agree closely with -0.20 mag and +1.80 mag from the visual orbit by Pan et al. (1992). For the binary system M_v = -0.32 $\pm$ 0.30 mag agrees with the Hipparcos absolute magnitude -0.4 mag (Gómez et al. 1998) within our error limits. From the usual relation between luminosity, effective temperature and radius we obtain $\rm R_A = 2.7 \pm 0.4\ R_\odot$ and $\rm R_B = 1.65 \pm 0.3\ R_\odot$ and a radii ratio of 1.64 $\pm$ 0.23 which agree with our binary flux fitting. The corresponding surface gravities are 4.15 $\pm$ 0.16 dex and 4.28 $\pm$ 0.20 dex for α And A and B, respectively. The spectroscopic surface gravity of α And A after correction for its helium deficiency is 3.86 (see Auer et al. 1966) which is smaller than that obtained from the evolutionary tracks.

5. Abundance analysis

It impossible to perform an accurate abundance analysis using the equivalent widths of α And A due to the severe blending produced by the substantial rotational velocities of both components. The secondary's contribution is not negligible; its lines compound the problem of blends. Fig. 5 shows a section of the spectrum of α And with the contribution from the secondary indicated by the dashed line. We fitted the iron lines using an abundance log(Fe/H) = -4.20. But if we used equivalent widths measured without considering the secondary's lines, then after correction for the binarity we find log(Fe/H) = -3.80, which overestimates the iron abundance in the primary's atmosphere. Even for Mn II which has lines only in the primary's spectrum, the neglect of the secondary results in the overestimate of the manganese abundance by 0.2 dex. Therefore we derived elemental abundances using synthetic spectrum calculations. Rotationally broadened spectra calculated for each component with the SYNTH and ROTATE codes (Piskunov 1992) were weighted according to the model flux ratios, shifted by the corresponding orbital velocities, added, and compared with the observations.

When we measure several relatively clean lines of the same atomic species for the primary, our abundance error estimate is similar to that for a single star. But for the secondary the formal error of any abundance determination is large even for spectra with high S/N. For a small spectral region around λ4960, we obtained a 'pure' secondary contribution by subtracting the

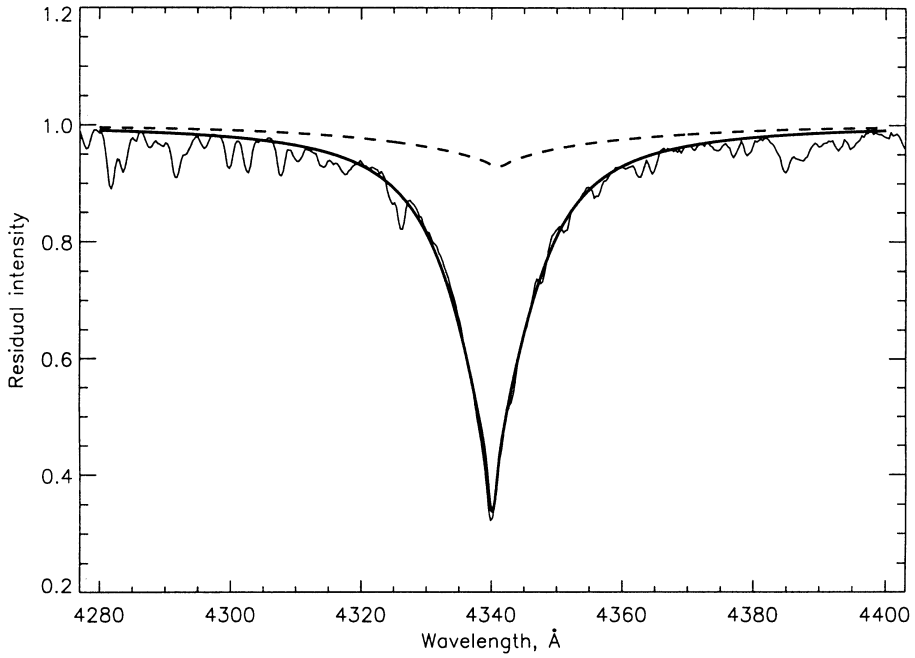

Fig. 3. A comparison between the observed and the computed Hγ line profiles. The contribution from the secondary is shown by dashed line.

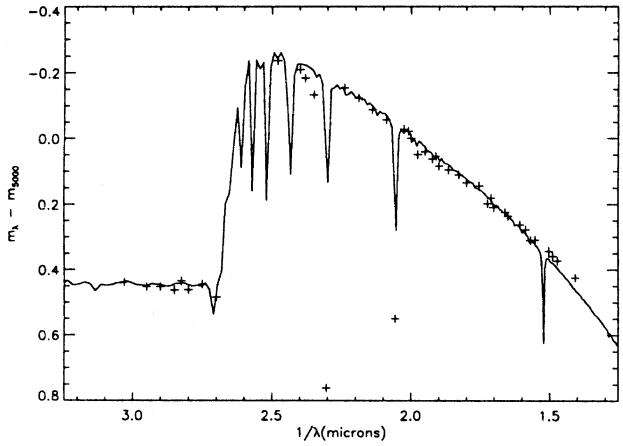

Fig. 4. A comparison between observed (pluses) and computed (solid line) spectrophotometry.

synthetic spectrum corresponding to the primary (see Sect. 2), then shifted each residual spectrum to the laboratory wavelength scale, and obtained an average spectrum (Fig. 6) which contains four Fe I line and a Ba II line. The best fit to the observations is shown by the thick line. For the Ba II line we also include two synthetic profiles with abundances ± 0.25 dex from the best fit value. The difference between profiles is about $\pm 0.1\%$ which roughly corresponds to the error of the residual intensity of this spectrum. This is our best case with the large S/N ratio produced by the averaging of 8 spectra. Usually we have just one spectrum per region. Hence the formal error of the secondary's abundances is not less than ± 0.3 dex. The atomic data for synthetic spectrum calculations were extracted mainly from VALD. For a few spectral lines without values in VALD we used other sources (see below in the results of the individual elements). It is impossible to derive microturbulent velocities for both components using equivalent widths. Thus we use zero microturbulence for the primary and 1.2 km s^{-1} the value for 112 Her B (Ryabchikova et al. 1996) for the secondary.

Table 3 presents our final derived abundances for α And A and B and those by Ljubimkov & Polosukhina (1988–LP), the most recent study where the authors used nearly the same atmospheric parameters for the primary as we did. Also we include photospheric abundances of two other binary systems with hot HgMn primaries and the most recent solar photospheric abundances (Grevesse et al. 1996). For κ Cnc which recently was found to be a SB2 system (Ryabchikova et al. 1998) all but the Xe abundance are from Adelman (1994). For 112 Her A, B the abundances are from Ryabchikova et al. (1996).

Helium. The helium abundance was obtained using five He I lines $\lambda\lambda$ 4121, 4471, 4713, 5016, and 6678. Fig. 7 compares the observed and the calculated spectra near the strongest observed line He I λ4471. A discrepency between the observed and calculated line profiles may not to be due to an inadequate broadening theory for the triplet neutral helium lines. If we fit the line wings, then the calculated line core is too strong. The same behaviour of triplet helium lines was observed in the hot star Feige 86 showing similar peculiarities in its spectrum – P, Pt, Au, Hg overabundances (Bonifacio et al. 1995). Hence we tried to obtain the same equivalent widths. For singlet helium lines our fits are better. With the substantial rotation of the primary it is impossible to study the isotopic anomaly in ^{3}He/^{4}He, observed in the hot HgMn stars κ Cnc and HD 182308 (Zakharova & Ryabchikova 1996).

Carbon and Oxygen. The primary's carbon abundance was calculated using the C II lines $\lambda\lambda$3918, 3920, and 4267. Carbon is deficient in α And A as it is in κ Cnc and to a larger degree in 112 Her A. The oxygen abundance was obtained from the O I λ3947 doublet. Oxygen is also deficient compared to the solar

Table 3. α And abundances (log N/H).

	This work		LP (1988)	κ Cnc	112 Her	112 Her	Sun
Species	Primary	Secondary	Primary	Primary	Primary	Secondary	
He I	-2.01±0.08 (5)			-2.26	-2.43		(-1.01)
C II	-3.88±0.10 (3)		-3.53	-3.97	-5.36:		-3.45
O I	-3.58: (1)		-3.53		-3.36:		-3.13
Mg II	-4.98±0.10 (3)	-4.4:		-5.17	-5.56	-5.25	-4.42
Si II	-4.38±0.10 (6	-3.9	-4.90	-4.48	-5.05		-4.45
Si III	-4.38: (1)			-4.47	-4.82:		-4.45
P II	-4.78±0.20 (12)			-4.73	-4.71		-6.55
P III	-4.83: (1)			-4.77	-4.80		-6.55
S II	-5.50: (2)			-5.56	-5.84		-4.67
Ca I		-6.2		-5.49	-4.55:	-6.45	-5.64
Ca II	-5.5±0.1 (6)		-5.69	-5.67			-5.64
Ti II	-6.68±0.10 (6)	-7.0:	-6.22	-6.82	-6.30	-7.06	-6.98
Cr II	-6.00±0.15 (11)	-6.0:	-5.67	-6.42	-6.50	-6.16	-6.33
Mn I	-3.70±0.15 (2)	-6.1:	-3.53	-4.39	-4.74	-6.51	-6.61
Mn II	-3.76±0.20 (30)		-4.45	-4.45	-4.91	-5.97	-6.61
Fe I	-4.20±0.15 (2)	-4.2±0.3	-3.21	-4.49	-3.55	-4.41	-4.50
Fe II	-4.22±0.10 (17)	-4.2±0.3	-4.18	-4.57	-3.60	-4.43	-4.50
Ni I		≤-5.5				-5.18	-5.75
Ni II	-5.98: (1)			-6.18	-6.07	-4.97	-5.75
Ga I	-4.83: (1)						-9.12
Ga II	-4.66±0.10 (4)		-4.73	-4.75	-5.27		-9.12
Sr II	-8.1: (1)	-8.8		-8.54	-8.57:	-8.67	-9.03
Y II	-7.7: (3)			-8.33	-8.04:	-8.67	-9.76
Zr II	≤-8.0 (3)				-7.74		-9.40
Xe II	-4.90±0.10 (3)			-4.68	-5.78		-9.77
Ba II		-8.75±0.25					-9.78
Hg II	-6.03: (1)		-5.40	-5.98	-5.98		-10.83

value. The difference between our carbon abundance and that of LP is due to the C II λ4267 doublet from which LP obtained a greater abundance by 0.5 dex than from two other lines.

Magnesium and Silicon. The magnesium abundance in α And A was obtained from three Mg II lines, $\lambda\lambda$4384, 4428, and 4481 while only the last line was used in the secondary. Fig. 7 compares the observed and computed spectra for Mg II λ4481 with the secondary's contribution indicated by a dashed line. Magnesium is deficient in the primary's atmosphere and seems to have a solar abundance in the secondary. Magnesium deficiencies are typically seen in hot HgMn stars.

The primary's silicon abundance was obtained from six Si II lines, $\lambda\lambda$3853-56-62, 4128-31 and 6347, and Si III λ4567. For α And B we mainly used Si II λ6347 observed at different orbital phases. Fig. 8 shows the observed and computed spectra near λ6347 for phase 0.14. Fig. 5 contains the fit for Si III λ4567. Our silicon abundance in α And A is slightly greater that of LP. They used ξ = 3 km s^{-1} which is a reason for their lower abundances.

Phosphorus and Sulphur. The phosphorus abundance in α And A exceeds the solar by 1.8 dex and coincides with those of κ Cnc and in 112 Her A. Only one P III line λ4222 was used to estimate the phosphorus abundance, and its result agrees with that from the P II lines.

The sulphur abundance in α And A is found from the S II lines, λ4153.07 and λ4162.66 of multiplet 44. Although both lines are blended and the final abundance is slightly uncertain, an underabundance of this element is definite; it is of the same order as was obtained for κ Cnc and 112 Her A. Sulphur deficiencies are characteristic of most HgMn stars (see Table 6 in Ryabchikova et al. 1996).

Calcium. It is difficult to use the resonance Ca II λ 3933 line for abundance determinations in both components due to the impossibility of a good theoretical fit in LTE for $T_{\rm eff}$ close to 8000 K and the poor theoretical representation of the high members of Balmer line profiles which influence the Ca II K line profile. Thus for α And A we used the subordinate Ca II lines, $\lambda\lambda$4489, 4721, 4800, 5001, 5020, and 5021. Although they are blended, synthetic spectrum calculations show good fits for all lines with log(Ca/H) = -5.5. LP obtained a slightly lower abundance using only the Ca II K line. If we neglect the hydrogen lines we get a good fit for this region with log(Ca/H) between -5.1 and -5.3 for the primary and log(Ca/H) around -6.0 for the secondary. Stark damping constants for the Ca II K line were from Dimitrijević & Sahal-Bréchot (1993). A slightly smaller Ca abundance for the secondary fits a wide feature in the secondary's spectrum which is a blend of Ca I λ4226 and a few strong Fe I lines (see Fig. 9). The Ca abundance in the primary is similar to that in κ Cnc and

is close to the solar value while the secondary is Ca-deficient like 112 Her B.

Iron-group elements. The abundance of titanium in the primary was obtained with six lines: $\lambda\lambda$4163.65, 4468.51, 4501.27, 4549.62, 4563.75, and 4572.00, the last three of which were used for the secondary's determination (see Fig. 5). The primary's iron abundance is based on two very strong Fe I lines, λ4045.81 and λ4383.55, and 20 Fe II lines mainly belonging to multiplets 27, 28, 37, and 38. The chromium abundance was derived using Cr II lines from the multiplets 30, 31 (partially blended lines), and 44 (see Fig. 5). The iron abundance for the secondary was obtained mainly from the Fe I lines near λ4957.5, which we used for RV measurements.

The primary's abundances of titanium, chromium, and iron are greater than solar by 0.3 dex as are the secondary's values within the expected errors, but titanium is perhaps slightly less abundant, as it is in 112 Her A, B. While iron is close to the solar value in α And A, B and practically solar in κ Cnc and 112 Her B it is 0.9 dex overabundant in 112 Her A. Our iron abundance from Fe II lines agrees with the value obtained by LP. Their great overabundance from Fe I lines is due to ignoring blends.

As expected manganese is the most overabundant iron-group element in the primary and nicely follows the temperature dependence for HgMn stars (e.g., Smith & Dworetsky 1993). Together with another hot HgMn star HR 6997, α And A is the richest in manganese. The large primary abundance makes possible to measure the strongest lines of Mn I $\lambda\lambda$4034.48 and 4041.36 (see Fig. 11). As manganese lines exhibit large hyperfine splittings, many strong Mn II lines have not used in previous abundance analyses. Holt et al.'s (1999) measurements of hyperfine structure now mean we can consider using strong Mn II lines such as $\lambda\lambda$4136, 4206, and 4259. Fig. 10 compares the observations and calculations with (thick line) and without (dotted line) hyperfine splitting in the spectral region $\lambda\lambda$4240–4277.

It is only possible to estimate the secondary's manganese abundance with the strongest Mn I lines of multiplets 1 and 5. Fig. 11 compares the observed and computed binary spectra in the spectral region $\lambda\lambda$4030–4050. A dotted line shows a synthetic spectrum calculated with the same manganese abundance for both stars log(Mn/H) = -3.8 while the thick line represents synthetic spectrum calculations with the abundances from Table 3. The secondary is less overabundant in manganese, which again agrees with the results for other HgMn binaries. LP obtained much a smaller manganese abundance with similarly sized equivalent widths. We used their equivalent widths and oscillator strengths and our model. The result for their ξ = 3 km s^{-1} is log(Mn/H) = -4.05 $\pm$ 0.38, which is 0.4 dex greater than the result of LP.

Only one Ni II line λ4067 may be used for a nickel abundance determination. Ni is slightly underabundant in the primary as it is in κ Cnc and in 112 Her A. An upper limit for the nickel abundance in the secondary shows the star could be slightly overabundant.

Gallium. Gallium is the most peculiar element in the primary's atmosphere. We used four Ga II lines $\lambda\lambda$ 4251, 4254, 4262,

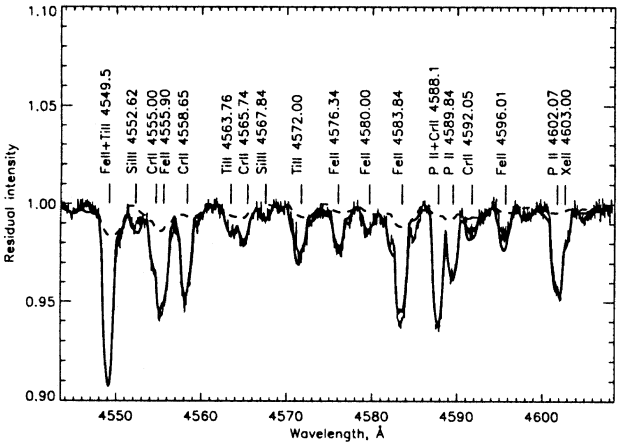

Fig. 5. The spectrum of α And centered at 4575 Å. A binary synthetic spectrum is shown by the thick line. The contribution from the secondary spectrum is indicated by dashed line. Line positions are shown for the primary.

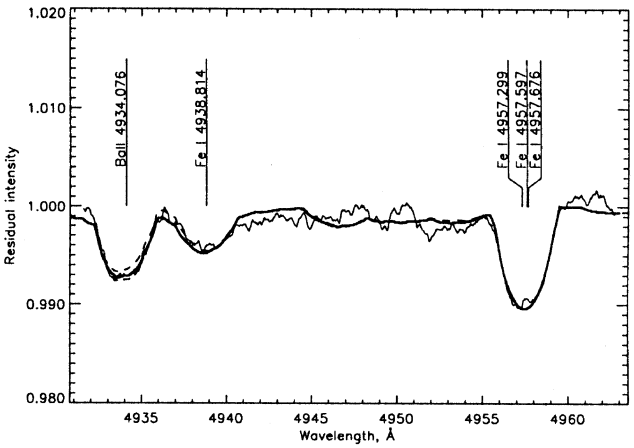

Fig. 6. Part of the secondary's spectrum after subtraction of the primary's. A calculated spectrum with the adopted secondary's abundances is shown by the thick line. For the Ba II line dashed lines are for values of the adopted Ba abundance $\pm$0.25 dex.

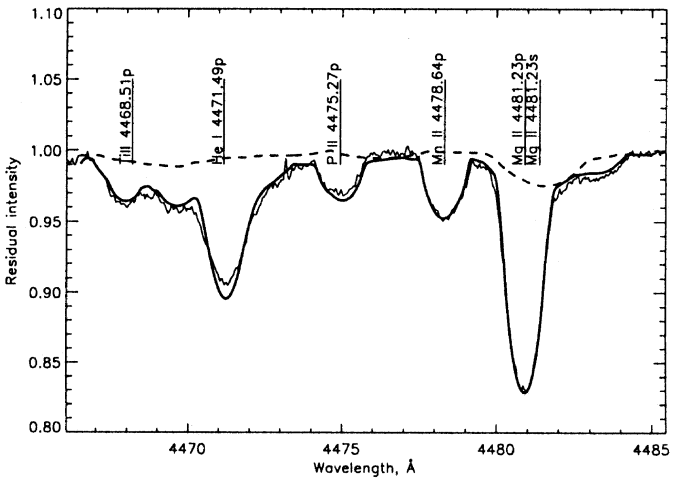

Fig. 7. The same as in Fig. 5 for the $\lambda\lambda$4465–4485 spectral region. Line positions are shown for the primary (p) and the secondary (s).

and 6334. The first three lines lack significant hyperfine splitting (Isberg & Litzen 1985), while for the last line we used hyperfine splitting data from Lanz et al. (1993). The abundance difference between the blue and the red lines does not exceed 0.1 dex. We do not use Ga II λ4255 due to its significant hyperfine splitting (Isberg & Litzen 1985) which may be seen in Fig. 11, where three Ga II lines, λ4251, 4254, and 4262 are fitted very nicely to the observations, while the calculated Ga II λ4255 is much weaker than the observed feature. Of two observed Ga I lines, only λ4033 is suitable for an abundance estimate. It is blended with a strong Mn I line. Still its gallium abundance is only slightly less than that from the Ga II lines. Comparisons between the observed and computed spectra for Ga I λ4034 and for Ga II λ6334 are shown in Figs. 11 and 8, respectively. Takada-Hidai et al. (1986) obtained log(Ga/H) = -5.6 from the equivalent widths of the resonance UV Ga II and Ga III lines. A difference between optical and UV abundances is typical for the most HgMn stars (Takada-Hidai et al. 1986, Smith 1996). Our calculations clearly showed that hyperfine structure which Smith believed to be one of the reasons for the observed descrepancy cannot explain it at least for α And. Smith also discussed the possibility of gallium atmospheric stratification which does not work for α And. According to Takada-Hidai et al. (1986) both Ga II λ1414 and Ga III λ1495 give practically the same Ga abundance while these values should be different if gallium is stratified in a stellar atmosphere (Smith 1996). Moreover the gallium abundances from **all** Ga II lines are identical in a stratified atmosphere.

Strontium, Yttrium, Zirconium. These three *s*-process elements are overabundant in the atmosphere of the primary. A comparison between the observed and best-fit computed spectra for Sr II λ4215 is shown in Fig. 9, and the same for Y II in Fig. 12. The strontium abundance in the secondary is close to solar.

Xenon. Xe II lines appear in the spectra of some hot HgMn stars. Our analysis is based on three Xe II lines $\lambda\lambda$4603, 4844, and 4973. We used oscillator strengths from Ryabchikova & Smirnov (1989) for the first two lines and from Iriarte et al. (1990) for the third line. The κ Cnc Xe abundance in Table 3 is from Ryabchikova & Smirnov (1989). The Xe abundance in α And A is nearly the same as in κ Cnc and greater than in 112 Her A by 0.9 dex.

Barium. Barium lines such as λ4934 are seen only in the secondary spectrum (see Fig. 6). The deduced barium abundance is about 1.0 dex greater than solar, and together with the calcium deficiency suggest we classify α And B as a metallic-line star.

Mercury. The mercury abundance is based on the analysis of the strongest Hg II line λ3984. The large rotational width of the line which exceeds the isotopic shift by more than three times makes it is impossible to study in detail the isotopic composition. Our calculations using the procedure proposed by Smith (1997) shows that isotopic-mix parameter *q* does not exceed 0.25. Thus the Hg isotopic composition in the atmosphere of α And A is close to terrestrial. Our value fits nicely the temperature dependence of *q*-parameter found by Smith (1997). The

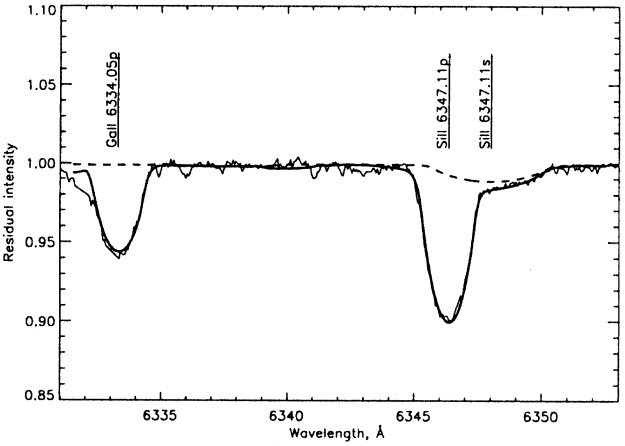

Fig. 8. The same as in Fig. 7 for the $\lambda\lambda$6630–6650 spectral region.

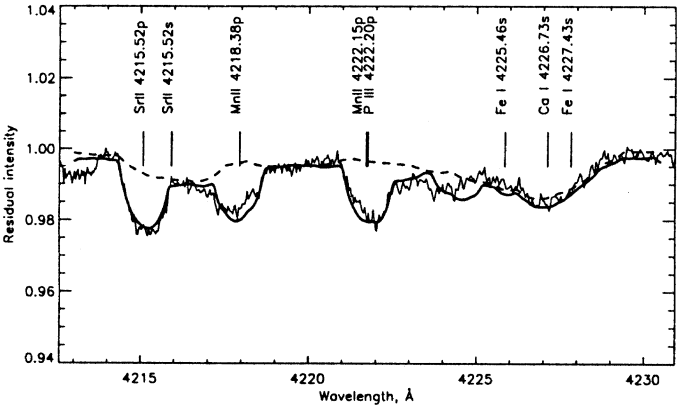

Fig. 9. The same as in Fig. 7 for the $\lambda\lambda$4213–4230 spectral region.

mercury abundance in α And A coincides with the abundances of this element both in κ Cnc and in 112 Her A.

We have three spectra in the region of Hg II λ 3984 line, and found a possible variability of the line profile. Fig. 12 compares the observed and the computed binary spectrum with the abundances from Table 3 for all three exposures. The most natural explanation of the observed profile variations is an inhomogeneous mercury distribution over the stellar surface. If it is supported by further observations then it will be the first indication for a spotty structure in HgMn stars. Where we have multiple spectra, we do not find any other lines to be variable. This topic is further investigated by Adelman, Gulliver & Ryabchikova (1999).

6. Some final comments

Based on our experience we recommend that investigators who are planning spectroscopic investigations of binary stars consider obtaining 1) high dispersion spectra with very high S/N ratios ($\geq$ 300) to make it easier to separate the two components and 2) more than one spectrum per region with different radial velocity separations of the two components to be able to verify a proper division. Although convention wisdom does not indicate a need for the obtained high dispersion spectra for

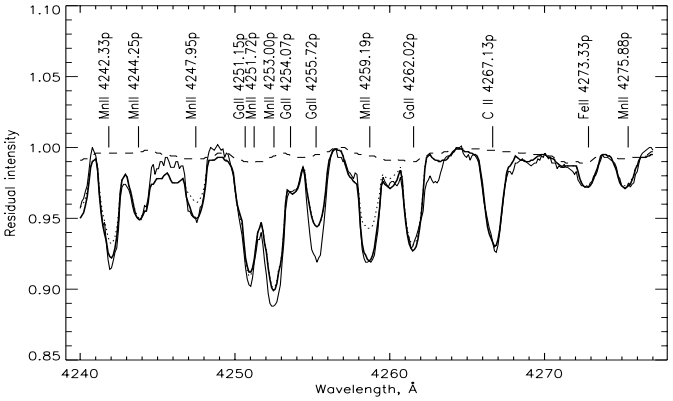

Fig. 10. The same as in Fig. 7 for the $\lambda\lambda$4240–4277 spectral region. Synthetic spectrum calculations with log(Mn/H) = -3.8 taking into account hyperfine splitting are shown by the thick line. Calculations without hyperfine splitting are shown by the dotted line.

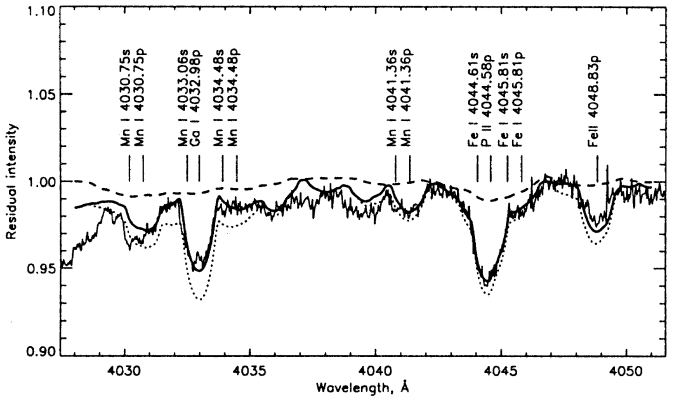

Fig. 11. The same as in Fig. 7 for the $\lambda\lambda$4028–4051 spectral region. Synthetic spectrum calculations with log(Mn/H) = -3.8 for both components are shown by the dotted line.

a star like α And having such spectra aided the analysis.

Acknowledgements. We thank Dr. A. Gómez for sending us a preprint of his paper. We also acknowledge the use of the VALD and SIMBAD data bases. We appreciate the help of Dr. Austin Gulliver in reducing rapidly the 1998 DAO spectrograms. TAR acknowledges financial support from the Russian Federal Program "Astronomy" grant 1.4.1.5. SJA thanks Dr. James E. Hesser, Director of the Dominion Astrophysical Observatory for the observing time used to obtain the DAO spectra of α And and The Citadel Development Foundation for several grants which supported in part this collaboration.

References

Abt H.A., Snowden M.S., 1973, ApJS 25, 137
Adelman S.J., 1994, MNRAS 266, 97
Adelman S.J., Gulliver A.F., Ryabchikova T.A., 1999, in preparation
Adelman S.J., Pyper D.M., 1983, A&A 118, 313
Adelman S.J., Ryabchikova T.A., Davydova E.S., 1998, MNRAS 297, 1
Aikman G.C.L., 1976, Publ. Dominion Astrophys. Obs. 14, 379

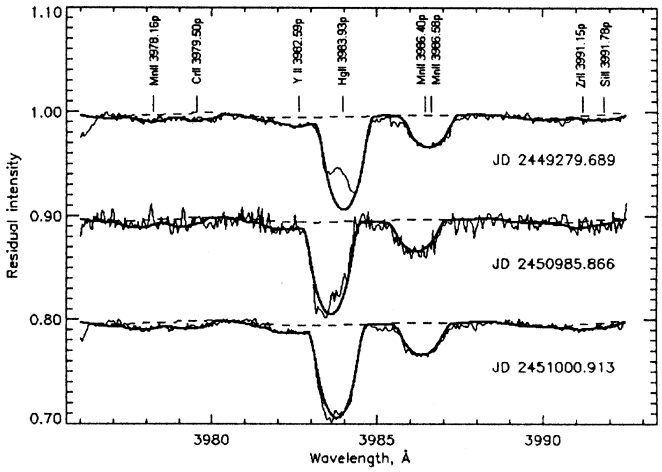

Fig. 12. The same as in Fig. 7 for the λ3984 spectral region for three different DAO exposures. Line positions are shown for the first spectrum.

Auer L.H., Mihalas D., Aller L.H., Ross J.E., 1966, ApJ 145, 153
Babu G.S.D., Shylaja B.S., 1981, Ap&SS 79, 243
Baker R.H., 1908, Pub. Allegheny Obs. 1, 17
Bonifacio P., Castelli F., Hack M., 1995, A&AS 110, 441
Derman I.E., 1982, Ap&SS 88, 135
Dimitrijević M.S., Sahal-Bréchot S., 1993, JQSRT 49, 157
ESA 1997, The Hipparcos Catalogue, ESA SP-1200
Flower P.J., 1996, ApJ 469, 355
Glushneva I.N., 1987, Russian Astron. J. 64, 601
Gómez A.E., Luri X., Grenier S., et al., 1998, A&A 336, 953
Grevesse N., Noels A., Sauval A.J., 1996, In: Cosmic Abundances. ASP Conf. Ser. 99, 117
Gulliver, A.F., Hill, G., Adelman, S.J., 1996, In: Adelman S.J., Kupka F., Weiss W.W. (eds.) ASP Conf. Ser. 108, Model Atmospheres and Spectrum Synthesis. ASP, San Francisco, p. 232
Heacox W.D., 1979, ApJS 41, 675
Holt R.A., Scholl T.J., Rosner S.D., 1999, MNRAS (in press)
Iriarte D., Di Rocco H.O., Raineri M., Reyna Almandos J., Gallardo M., 1990, J. Molec. Structure (Theochem) 210, 253
Isberg B., Litzen U., 1985, Phys. Scripta 31, 533
Khokhlova V.L., Aliev S.A., Rudenko V.M., 1969, Izv. Krymsk. Astrofiz. Obs. 40, 65
Kodaira K., Takada M., 1978, Ann. Tokyo Astron. Obs. 17, 79
Kurucz R.L., 1992, Rev. Mex. Astron. Astrofis. 23, 45
Lanz T., et al., 1993, A&A 272, 465
Ljubimkov L.S., Polosukhina N.S., 1988, Izv. Krymsk. Astrofiz. Obs. 80, 30
Ludendorff H., 1907, Astron. Nachr. 176, 327
Martin G.A., Fuhr J.R., Wiese W.L., 1990, NIST Standard Reference Data Base 24, Gaithersburg, MD 20899, USA
Pan X., Shao M., Colavita M.M., et al., 1992, ApJ 384, 624
Piskunov N.E., 1992, In: Glagolevskij Yu.V., Romanyuk I.I. (eds.) Stellar magnetism. Nauka, St. Petersburg, p. 92
Piskunov N.E., Kupka F., Ryabchikova T.A., Weiss W.W., Jeffery C.S., 1995, A&AS 112, 525
Ryabchikova T.A., Smirnov Yu.M., 1989, Astron. Tsirk. N1534, 21
Ryabchikova T.A., Zakharova L.A., Adelman S.J., 1996, MNRAS 283, 1115
Ryabchikova T., Kotchukhov O., Galazutdinov G., Musaev F., Adelman S.J., 1998, Contrib. Astron. Obs. Skalnate Pleso 27, No. 3, 258

Schaller G., Schaerer D., Meynet G., Maeder A., 1992, A&AS 96, 269
Shallis M.J., Blackwell D.E., 1979, A&A 79, 48
Shallis M.J., Baruch J.E.F., Booth A. J., Selby M.J., 1985, MNRAS 213, 307
Smith K.C., 1996, A&A 305, 902
Smith K.C., 1997, A&A 319, 928
Smith K.C., Dworetsky M.M., 1993, A&A 274, 335
Takada-Hidai M., Sadakane K., Jugaku J., 1986, ApJ 304, 425
Tokovinin A., 1992, In: McAlister H.A., Hartkopf W.I. (eds.) ASP Conf. Ser. Vol. 32, Complementory Approaches to Double and Multiple Star Research. ASP, San Francisco, p. 573
Tomkin J., Pan X., McCarthy J.K., 1995, AJ 109, 780
Wahlgren G.A., Adelman S.J., Robinson R.D., 1994, ApJ 434, 349
Zakharova L.A., Ryabchikova T.A., 1996, Astronomy Letters 22, 152